A Theoretical Study on the Paths of Photodissociation: CH_2=C=O → CH_2 + CO

Shinichi Yamabe[1a,c] and Keiji Morokuma*[1b,c]

*Contribution from the Department of Chemistry, Nara University of Education,
Takabatake-cho, Nara 630, Japan, The Institute for Molecular Science,
Myodaiji, Okazaki 444, Japan, and the Department of Chemistry,
The University of Rochester, Rochester, New York 14627. Received May 11, 1978*

Abstract: Molecular orbital and state correlation diagrams were examined for symmetric and nonsymmetric dissociation pathways of ketene in the ground and lower excited states. For the pathways allowed by symmetry ab initio calculations were carried out to determine the reaction paths. Four possible paths were found: the bent in plane path (all the atoms are in a plane but the oxygen atom deviates from the CH_2 molecular axis) and the bent out of plane path (the CH_2 molecular axis and CO are in a plane) with both the spin multiplicity of singlet and triplet.

I. Introduction

Ketene (CH_2=C=O) has been widely used as a photochemical source of methylene (CH_2). Recent evidences, primarily based on product analysis and quenching data, have suggested that both spin states (singlet and triplet) of CH_2 are formed by the photolysis of ketene in the 260–370-nm wavelength region.[2-6] Ethylene and carbon monoxide are the major products of the following widely accepted mechanism which is consistent with their quantum yield:[7-9]

$$CH_2CO \xrightarrow{h\nu} CH_2CO^* \longrightarrow CH_2 + CO \xrightarrow{CH_2CO} C_2H_4 + 2CO$$
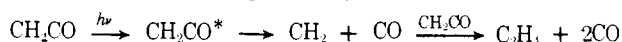
It is also known that an increase in the wavelength causes a decrease in the fraction of the singlet methylene and an increase in the fraction of the triplet[4] and that the quantum yield of CO depends on both pressure and temperature as well as on the wavelength.[7] To rationalize these results, a mechanism involving several processes such as the collision-induced intersystem crossing and internal conversion has been proposed.[9] Russel and Rowland suggested, based on the observed exchange of the radioactive ^{14}C in the course of dissociation, that a part of the singlet methylene was formed through an oxirene intermediate.[10] These results show that the overall photochemical mechanism is extremely complicated.

Electronic spectra of ketene have been reported and discussed, resulting in only uncertain assignments of absorption bands.[11-13] In addition, it is disputable whether the diffuse absorption spectra in the gas phase at the 260–470-nm range are caused by the predissociation or by the rotational structure coupled to a pseudocontinuum of a bound electronic state.[13]

Some ab initio theoretical calculations on the electronic structure of ketene have been carried out. Basch performed an MCSCF calculation for several electronic states along the C_{2v} dissociation path.[14] In order to obtain the equilibrium geometry, Del Bene carried out CI calculations for three excited states with the STO-3G minimal basis set.[15] She found a substantial C–C–O bending in each excited state. Similarly, Dykstra and Schaefer calculated the geometry of ketene in its excited state as well as in the ground state with a larger (double ς) basis set.[16] Pendergast and Fink searched the C_{2v} and bent dissociation paths in terms of the C–C distance within the SCF and limited CI framework.[17] In spite of these calculations information on photodissociation paths of ketene is still insufficient for the following reasons:

(1) The path of the highest symmetry (C_{2v}), i.e., the least motion path, is unfavorable both in the ground and low-lying excited states, as will be explained in the next section. Therefore, a calculation along such a path is unrealistic and chemically not instructive, no matter how accurate it is.

(2) Since the C_{2v} path is unfavorable, some geometrical relaxation has to be introduced to search a favorable path. For this purpose, one has to make a systematic examination of the correlation diagram, which has not been done.

(3) As the optimization of all degrees of freedom along the path is difficult, one must present a reasonable criterion for freezing unimportant degrees of freedom. As an obvious example, changing the C–H length of ketene in the course of the dissociation is not essential. In the same respect, it is not enough to change only the C–C bond length to describe the dissociation. The chemically intuitive correlation diagram suggested above provides a reliable ground for restricting some freedoms of optimization.

In the present paper we at first examine molecular orbital and state correlation diagrams for symmetric and nonsymmetric dissociation pathways of ketene in the ground and lower excited states. Guided by the diagrams, we then carry out ab initio calculations for the dissociation paths with proper symmetries.

II. Qualitative Description of Reaction Paths

The simplest and least motion dissociation path is the separation of CH_2 and C–O along the C–C–O axis, maintaining the C_{2v} symmetry. Figure 1 shows the MO diagrams for ketene and the products in the C_{2v} representation. There, a_1 is for a σ orbital, b_1 is for a π orbital which is perpendicular to the molecular plane, and b_2 is for a π' orbital which lies on the molecular plane and is antisymmetric with respect to the two hydrogen atoms. One can see that the lowest seven occupied MOs ($1a_1$ to $1b_2$) are common to both ketene and the two products. Thus it is convenient to consider explicitly only eight high-lying "active" electrons (filled circles) in constructing the correlation diagram, the ground state being $(7a_1)^2$-$(1b_1)^2(2b_2)^2(2b_1)^2$ for ketene and $(2b_2)^2(1b_1)^2(7a_1)^2(8a_1)^2$ for the products.

In Figure 2, the state correlation diagram along the C_{2v} reaction path is drawn for the ground and some low-lying states. The number for the "active" electrons is shown for each symmetry at both edges of the figure. By comparing these numbers between ketene and the products, one can tell directly whether the C_{2v} dissociation path is "allowed" or not. For instance, the $^1A_1$ ground state of ketene has a different set of numbers of electrons in three symmetries (2,4,2) from that of the products (4,2,2). Therefore, the C_{2v} reaction path in the ground state will have a high barrier and is forbidden. The $8a_1^2$ → $2b_1^2$ excited configuration of CH_2 with the ground state of CO has a (2,4,2) electron set and is the partner configuration for the $^1A_1$ ground state of ketene. Likewise, the low-lying excited states, $^{3,1}A_2$ and $^{3,1}A_1$, of ketene find their partner product states in higher energy levels.
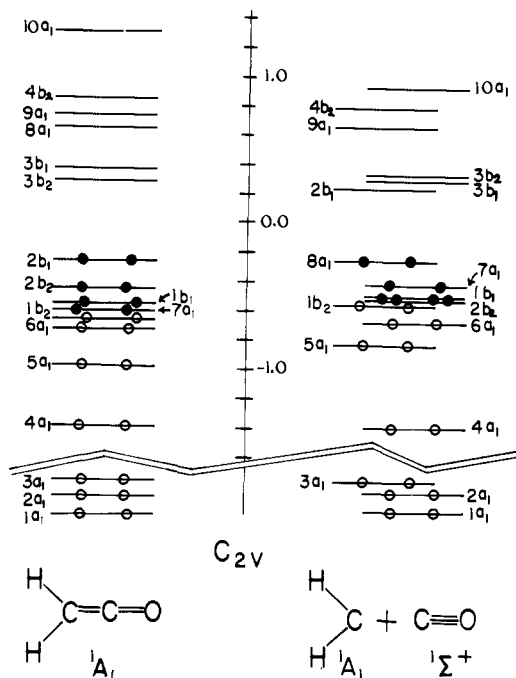
Figure 1. The MO energy levels of ketene, CH_2, and CO in their ground state calculated with the STO-3G minimal basis set. The geometrical parameters of ketene are taken from experiment[20] [$\angle HCH = 122.3°$, $R(C-H) = 1.079$ Å, $R(C-C) = 1.315$ Å, and $R(C-O) = 1.16$ Å] and those of the products are assumed to be the same as in ketene except for $R(C-O)$. The energy is in units of hartree = 627.5 kcal/mol. Filled circles denote "active" electrons which are used to construct the correlation diagram in Figure 2.
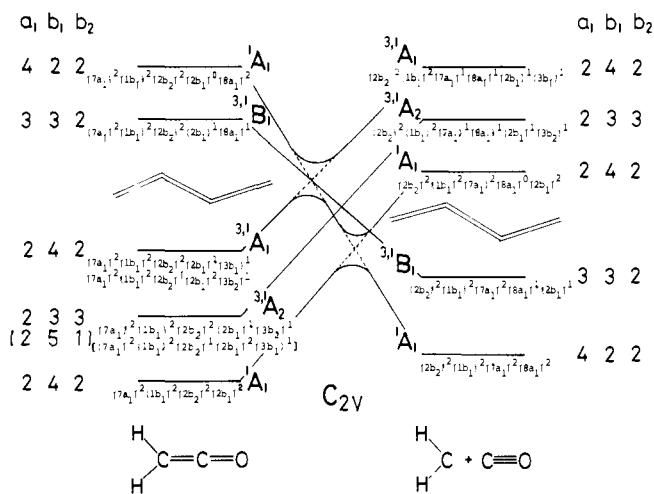

Figure 2. The state correlation diagram for the C_{2v} dissociation path of $CH_2CO \rightarrow CH_2 + CO$. At both edges, sets of numbers represent number of "active" electrons assigned to each irreducible representation. The electronic configuration shown below each state denotes a major configuration contributing to the state.

Thus the C_{2v} dissociation path is not allowed in *any* low-lying state. A deviation from the C_{2v} symmetry is required in order for the reaction to proceed easily. One possibility of such a deviation is a bent structure preserving the coplanarity of all the atoms which we call the path I "bent in plane". Another is a path involving a symmetric out of plane bending, which we call the path II "bent out of plane". In this the plane including OCC and the center of mass of H–H remains to be a symmetry plane. Both paths I and II have the C_s symmetry.

Shown in Figure 3 is the correlation diagram for the "bent in plane" process. In this symmetry, both a_1 and b_2 in C_{2v} become a' (symmetric or of σ type with respect to the molecular
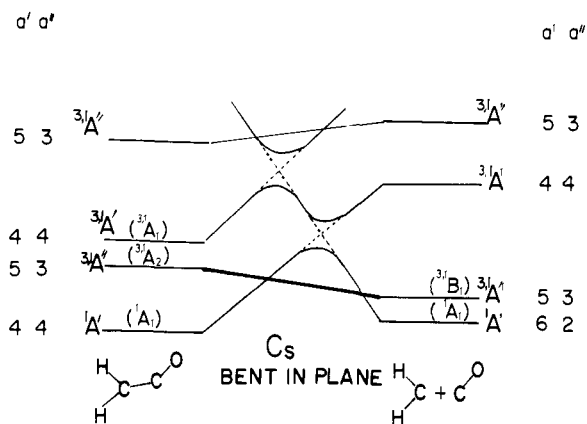

Figure 3. The state correlation diagram for the bent in plane dissociation path. The bold line denotes the allowed path. The assignment of eight electrons is according to the C_s symmetry, written at each edge of the figure. The states shown in the parentheses are for the C_{2v} symmetry.
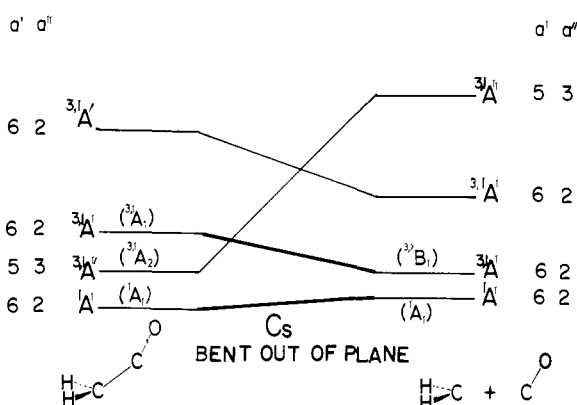

Figure 4. The state correlation diagram for the bent out of plane dissociation path. For notation, see Figure 3.

plane) and b_1 in C_{2v} becomes a'' (antisymmetric or of π type with respect to the molecular plane). The $^{3,1}A''$ states, which in C_{2v} were $^{3,1}A_2$ for ketene and $^{3,1}B_1$ for the products, find their partners among the lower states. Thus, the $^{3,1}A''$ paths are symmetry allowed in the bent in plane deformation. As will be mentioned later, the bent in plane $^{3,1}A''$ paths can be described in terms of a single electron configuration, which is essentially a $b_1 \rightarrow b_2$ ($\pi \rightarrow \pi'$) excitation for ketene and an (a_1 b_1) open-shell state for CH_2.

The correlation diagram of the bent out of plane path is shown in Figure 4. In this symmetry both a_1 and b_1 in C_{2v} are reduced to a' (symmetric with respect to the symmetry plane), while b_2 becomes a''. The ground state with six a' and two a'' electrons can be connected directly between ketene and the products. At the same time, the $^{3,1}A'$ ($^{3,1}A_1$ for C_{2v}) states of ketene find a new partner on the product side which was originally the $^{3,1}B_1$ state. As will be mentioned later, the lower excited $^{3,1}A'$ states can be described by a single electron configuration which is essentially a $b_1 \rightarrow b_1$ ($\pi \rightarrow \pi^*$) excitation for ketene and an (a_1 b_1) open-shell state for CH_2. Thus, the bent out of plane deformation makes the paths between the ground–ground and $^{3,1}A_1$–$^{3,1}B_1$ states allowed, while it keeps the reaction of the $^{3,1}A_2$ states forbidden.

Changes of other geometrical parameters such as the C–O bond length or the HCH angle do not have an effect on essential features of the correlation diagrams. In fact, their changes are very small throughout the dissociation as will be shown in the following sections.

In the following sections, we will investigate carefully four "allowed" photodissociation paths, i.e., the bent in plane paths
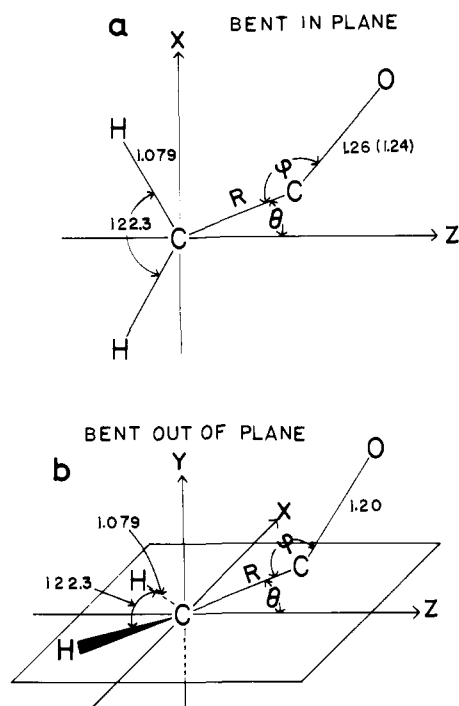
Figure 5. The geometrical parameters (R, θ, and ψ) and the coordinate taken for the (I) bent in plane dissociation path (a) and for (II) bent out of plane dissociation path (b). In (a), the C–O bond length, 1.26 Å, is for the $^3A''$ state and that in parentheses, 1.24 Å, is for the $^1A''$ state.[15]

(I) for both singlet and triplet A″ states and the bent out of plane paths (II) for both singlet and triplet A′ states. An emphasis will be placed on the direction in which the dissociation fragments, CH_2 and CO, separate.

III. Method of Calculation

To obtain the reaction path explained in the previous section, the SCF wave function for both singlet and triplet is calculated by the generalized restricted Hartree–Fock (GRHF) method[18] with the STO-3G minimal basis set.[19] The choice of this one-configuration wave function is based on the result of preliminary MC (multiconfiguration) SCF calculations, which indicated that one particular configuration dominated each state.

The geometrical parameters for (I) bent in plane and (II) bent out of plane paths are defined in Figures 5a and 5b, respectively. At a given C–C distance (R), two angles, θ and ψ, are simultaneously optimized. The geometry of the fragmental CH_2 is frozen to that of ketene taken from the experimental result in the ground state.[20] The C–O bond length is also fixed to the constant value shown in the figure, which is very close to that (1.128 Å[21]) of carbon monoxide. For the (I) bent in plane path all the atoms are located in the x–z plane, whereas for the (II) bent out of plane path two carbon atoms and oxygen atom are always in the y–z plane. The C–C bond length of the excited equilibrium geometry of ketene is taken from Del Bene's result.[15]

IV. Details of Reaction Paths

The results of the energy optimization along four types of dissociation paths are summarized in Figure 6. The change of energy along the bent in plane path for the triplet A″ ($\pi \rightarrow \pi'$) state is shown in Figure 6a-1. This curve shows a smooth change of the potential energy and the transition state is located at around $R = 2.0$ Å (D) with the calculated activation energy $\sim$33 kcal/mol. Being the result of an SCF calculation with a minimal basis set, the energy should not be taken too seriously. In Figure 6a-2, the bisector of the HCH angle is held
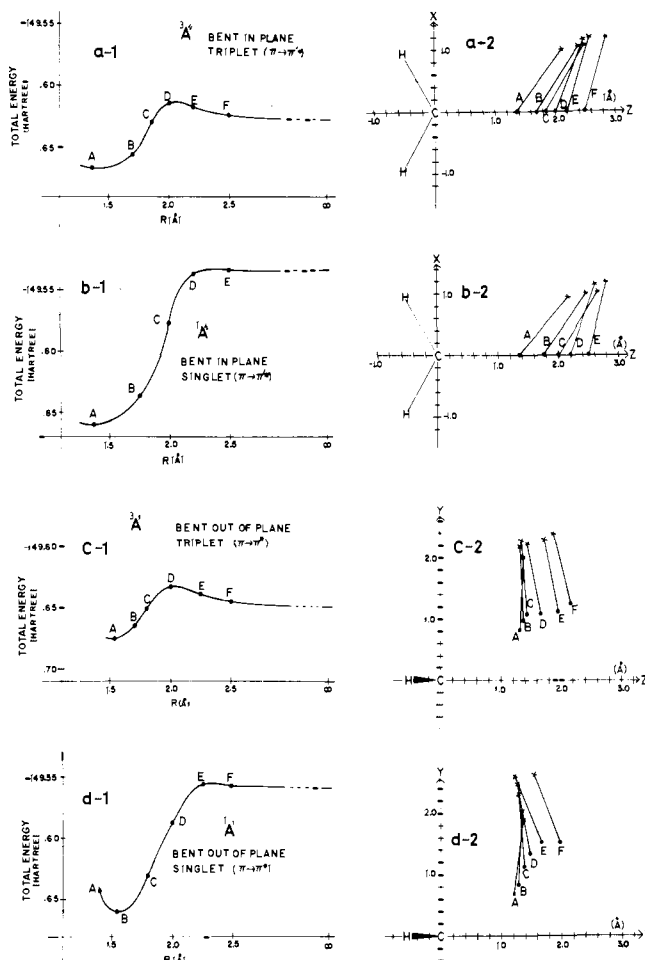

Figure 6. (a) Four reaction paths for photodissociation of ketene. The GRHF total energy along the optimized paths. (b) The optimized geometry at each R along the paths. The filled circle and the cross denote the carbon and the oxygen atoms of C–O, respectively.

on the z axis and the motion of the leaving C–O fragment in the $^3A''$ state is depicted. The geometry A is the optimized geometry of the $^3A''$ excited state of ketene and at F the two products are well separated with little interaction. Interestingly, only a small geometrical change except for the C–C distance is needed to describe the potential curve along the least energy pathway. It is worth noticing that the carbon atom of the leaving C–O remains on the z axis. In other words, θ is always zero throughout the bent in plane path, although two angles, θ and ψ, were simultaneously optimized. A nonzero θ, if it is deliberately taken, brings about a sharp destabilization. The interpretation for this behavior will be given in terms of the energy components in the next section. One can also see that the angle, ψ, becomes smaller along the proceeding of the dissociation, in particular, after the transition state (D) is passed. This result is also explainable by the energy decomposition scheme.

The energy change along the singlet A″ bent in plane path is shown in Figure 6b-1. Different from the $^3A''$, this state shows a monotonic increase in energy along the dissociation path. This appreciable ascent of the energy curve is attributed to the fact that the total energy of the $^1B_1$ CH_2 is calculated to be 66 kcal/mol above the $^3B_1$ CH_2, whereas the energy difference of ketene between $^1A''$ and $^3A''$ at the geometry A is 4 kcal/mol (by ignoring the small difference in their geometries). The large endothermicity apparently makes the energy maximum disappear. In consideration of the experimental ($^3A_2$–$^1A_2$) energy difference, 12 kcal/mol of the λ_{max} transition energy[12] of ketene, and the ($^1B_1$–$^3B_1$) energy dif-
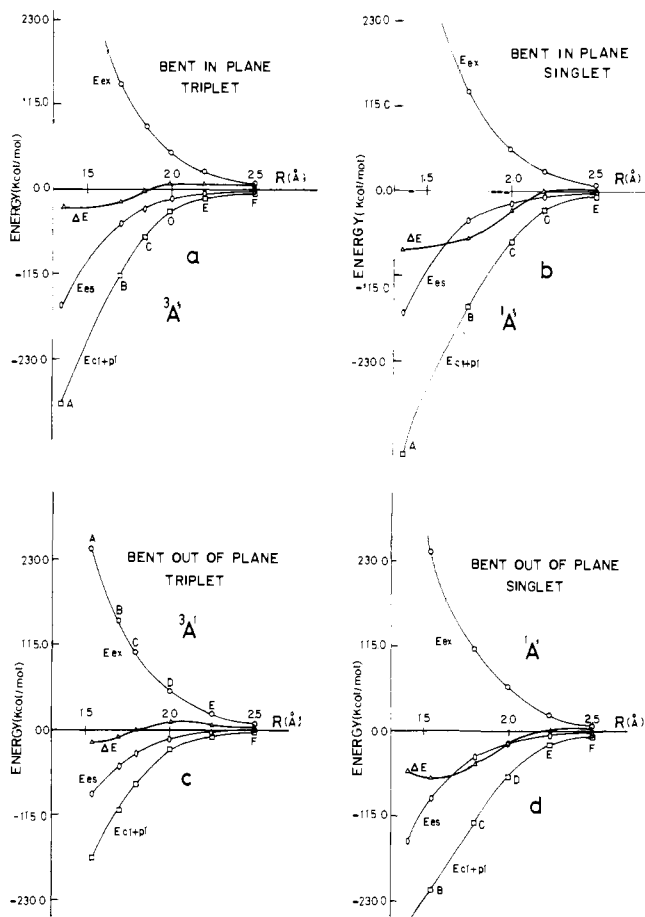
Figure 7. The change of energy components along four optimized paths for the recombination reaction $CH_2^* + CO \rightarrow CH_2CO^*$. The energy is negative when a stabilization takes place. $\Delta E = E_{es} + E_{ex} + E_{ct+pl}$.

ference of CH_2, 46 kcal/mol, of the rigorous CI calculation[22] (experimentally unknown), it is not clear whether the correct potential surface should have a barrier or not in the $^1A''$ path. The motion of the leaving C–O in the $^1A''$ path, as is shown in Figure 6b-2, is similar to that of the triplet.

In Figure 6c-1, the energy profile along the bent out of plane path for the $^3A'$ state is exhibited. The potential curve is very similar to that of the bent in plane triplet (Figure 6a-1) and has the transition state near $R \sim 2.0$ Å (D) with an activation energy ~ 28 kcal/mol. In Figure 6c-2, the dissociation path of $^3A'$ is displayed on the y-z plane, the plane defined by the bisector (the z axis) of HCH and CO. It is noticed that the geometry A, the optimized geometry for the $^3A'$ state of ketene, has a large θ (32°) in this calculation, as was also pointed out by Dykstra and Schaefer.[16] Along the dissociation path, θ increases appreciably from the geometry A to C and then decreases slowly from D (the transition state) to F. The change in ψ is not appreciable throughout the path.

Finally, the dissociation along the singlet bent out of plane path for the $^1A'$ state is followed in Figures 6d-1 and 6d-2. The potential curve ascends sharply as R is increased, as in the $^1A''$ bent in plane path (Figure 6a-1).[23] The leaving CO group tends to swing farther away from the CH_2 plane than in the triplet path (Figure 6c-2).

As a summary of the energy optimization for four dissociation paths, we note that the θ remains zero for the bent in plane paths, but, for the bent out of plane paths, θ increases until it reaches the transition state and decreases afterward. It is also noticed that ψ decreases slowly along the path and its change is largest near the transition state. The difference in the dissociation path due to the spin multiplicity is small for

the bent in plane case, but is more noticeable for the bent out of plane case.

V. Energy Decomposition along the Reaction Paths

The energy decomposition analysis of Morokuma et al. allows the interaction energy between molecules to be partitioned into chemically meaningful components: electrostatic, exchange, polarization, charge transfer, and their coupling terms.[24] The scheme has been applied to the interaction between a molecule in an excited state and a molecule in the ground state[24b] as well as between the ground-state molecules. To aid our interpretation of the reaction paths obtained in the preceding section, we carry out the analysis by considering the (reverse) paths as results of interaction between CH_2 ($^{3,1}B_1$) and the ground-state CO. At each point on the path the interaction energy ΔE (the energy difference between the complex and the isolated $CH_2 + CO$) is divided into chemically meaningful components: electrostatic (Coulombic) E_{es}, exchange E_{ex}, polarization E_{pl}, charge transfer E_{ct}, and their coupled E_{mix}. In the present paper, $E_{ct+pl} = E_{ct} + E_{pl} + E_{mix}$ will be calculated only as a group. A positive (negative) value of interaction corresponds to an repulsion (attraction).

In Figure 7, we show the results of the energy decomposition along the paths obtained in the preceding section. In all four cases the attractive electrostatic energy E_{es} is a slowly changing function of the C–C distance R. On the other hand, both the repulsive E_{ex} and the attractive E_{ct+pl} increase their magnitude rapidly as R decreases. This is because both terms are essentially proportional to the square of the overlap, which is extremely sensitive to the change in R. The importance of the delocalization term E_{ct+pl} in all these reactive cases is in a remarkable contrast with cases of weak interaction which is rarely dominated by the delocalization.[25]

Now we use the energy decomposition scheme to examine the reason why the least energy paths should follow those obtained in section IV. Table I shows calculations for the analysis. We found in section IV that the bent in plane paths retained $\theta = 0$ throughout the course of reaction. The calculation no. 1 corresponds to the optimized point C on the reaction path for $^1A''$. In no. 2 θ is taken to be 30° and all other geometrical parameters are assumed to be equal to those in no. 1. A comparison between the two shows the origin of stability for $\theta = 0$. The geometry with $\theta = 0$ is favorable mainly due to a favorable E_{ct+pl}. The CH_2 has a half-occupied σ ($8a_1$) orbital along the z axis (Figure 5a). The interaction of this orbital with CO orbitals will be the largest when the carbon atom is on the z axis, i.e., $\theta = 0$. The same trend can be observed by comparing no. 7 (optimized) with no. 9 ($\theta \neq 0$) for the $^3A''$ bent in plane path. A comparison among no. 7 (optimized ψ), no. 6 ($\psi < \psi_{opt}$), and no. 8 ($\psi > \psi_{opt}$) gives an interpretation for $\psi_{opt} \sim 112°$. Near ψ_{opt}, E_{ex} prefers a small ψ in order to minimize the CO σ–methylene C σ overlap, but does not want to make ψ too small (to avoid the CO π–methylene H overlap). On the other hand, E_{ct+pl} prefers the CO σ–methylene C σ overlap. A balance between E_{ex} and E_{ct+pl} apparently resulted in ψ_{opt}.

The change of θ along the triplet bent out of plane path will now be examined (no. 10–15). Here one notices that a larger θ makes a repulsion (E_{ex}) more repulsive and an attraction ($E_{es} + E_{ct+pl}$) more attractive. A balance between them gives θ_{opt}. The effect of the repulsion is more predominant for a smaller R, and therefore the value of θ_{opt} decreases as a function of R.

VI. Concluding Remarks

In this study an ab initio calculation of the photodissociation of ketene, based on the consideration of the correlation diagram, is presented. As a result of the energy optimization, four different paths, along which ketene dissociates smoothly to the products ($^{3,1}B_1$ CH_2 and ground-state C–O), are obtained. The

Table I. Calculated Results of Energy Decomposition for $CH_2 + CO \rightarrow CH_2CO$

no.	type	optimization[a]	R, Å	θ, deg	ψ, deg	ΔE[b]	E_{es}	E_{ex}	E_{ct+pl}
1	bent in plane	C	2.00	0.0	122.1	−26.8	−14.5	57.7	−69.6
2	singlet (¹A″)	no	2.00	30.0	122.1	−9.7	−15.0	59.7	−54.4
3	bent in plane	no	1.70	0.0	112.0	−16.4	−42.0	135.8	−110.2
4	triplet (³A″)	B	1.70	0.0	123.2	−18.1	−46.1	144.1	−116.2
5		no	1.70	0.0	134.0	−15.8	−50.5	154.5	−119.9
6		no	2.00	0.0	96.0	10.8	−11.5	49.6	−27.1
7		D	2.00	0.0	111.6	8.1	−12.7	49.8	−29.1
8		no	2.00	0.0	127.0	10.7	−14.3	54.4	−29.5
9		no	2.00	30.0	111.6	15.5	−13.6	52.8	−23.8
10	bent out of plane	no	1.80	30.0	121.7	−0.6	−32.3	105.4	−73.6
11	triplet (³A′)	C	1.80	36.6	121.7	−0.9	−32.8	106.1	−74.3
12		no	1.80	43.0	121.7	−0.7	−33.2	107.0	−74.5
13		no	2.00	26.0	112.0	10.5	−13.2	51.0	−27.2
14		D	2.00	33.1	112.0	10.4	−13.4	51.4	−27.7
15		no	2.00	40.0	112.0	10.6	−13.8	52.4	−27.9

[a] C, D, and B are optimized geometries in each reaction path shown in Figure 6. "No" refers to assumed models taken for comparison.
[b] Energies are in kcal/mol.

present calculation is made with a small basis set (STO-3G) and energetics shown here should be considered merely qualitative.

$^3B_1$ methylene can be formed via either bent in plane or bent out of plane path. If the reaction initiates from the π-π^* (A_1) excited state of ketene, it should follow the bent out of plane path. If it is from the π-π' (A_2) excited state of ketene, it will proceed through the bent in plane path. Energetics along the paths are rather similar, and the actual path or paths will depend on which triplet one reaches via intersystem crossing from the singlet state or via sensitization. $^1B_1$ methylene is also obtained as a dissociation limit from the ketene of both $^1A_2$ and $^1A_1$ states. In fact, it is suggested that the photolysis of ketene by the wavelength of 200–313 nm yields the $^1B_1$ CH_2.[26] The total energy curves of triplet paths are expected to have maxima, while the singlet paths would be energetically simply uphill, or would have a small barrier.

It is not easy to consider global aspects of the potential energy surfaces.[27] If ketene in the C_{2v} ground state is excited vertically to the A_2 singlet or triplet state, it will bend in plane as the C–C bond is stretched. It appears that there are no other potential surfaces nearby in this case. When ketene is excited to the A_1 singlet or triplet state, it will start bending out of plane. The $^{1,3}A_2$ states, which were lower in energy than $^{1,3}A_1$ in the C_{2v} symmetry,[16] are unstabilized in the out of plane bending and will cross over $^{1,3}A_1$. An asymmetric vibration couples the A_1 and the A_2 state. Most of trajectories which started from A_1 will follow the $A_1(A')$ surface, but there is a chance that some trajectories switch over to the $A_2(A'')$ surface, which will introduce a bending in plane as the dissociation proceeds.

The route for the dissociation $CH_2CO \rightarrow CH_2(^1A_1) + CO$ has not been traced in this work, but as is shown in Figure 4, it will take a bent out of plane path. Experimentally thermodynamic decomposition is well known for the isoelectronic diazomethane ($CH_2N_2 \rightarrow CH_2 + N_2$). One would expect that the reaction would be accelerated by the out of plane bending and would follow a bent out of plane path.

Finally, the conclusions obtained in this work are as follows.

(1) There are four possibilities for ketene to dissociate photochemically into $CH_2 + CO$: through the bent in plane path and the bent out of plane path with the spin multiplicity of singlet and triplet.

(2) For the bent in plane path the carbonyl carbon atom remains on the symmetry axis of CH_2. The carbonyl CO axis

becomes more and more perpendicular to the CH_2 symmetry axis as the C–C bond is stretched.

(3) For the bent out of plane path the deviation of the carbonyl carbon atom and the carbonyl CO axis takes place simultaneously.

(4) Both the bent in plane and the bent out of plane triplet path have the transition state at around the C–C bond length of 2.0 Å.

(5) The spin multiplicity does not drastically affect the trace of reaction paths.

(6) The geometrical change along the reaction paths is interpreted in terms of energy components for reverse recombination reaction: $CH_2^* + CO \rightarrow CH_2CO^*$. At smaller C–C distances the relative orientation appears to be determined in such a way that the orbital overlap between CH_2 σ and C–O orbitals is chosen to maximize the charge transfer attraction without giving rise to a sharp exchange repulsion.

References and Notes

(1) (a) Nara University of Education; (b) The Institute for Molecular Science; (c) The University of Rochester.
(2) W. Kirmse, "Carbene Chemistry", Academic Press, New York, N.Y., 1964.
(3) B. A. DeGraff and G. B. Kistiakowsky, J. Phys. Chem., 71, 3984 (1967).
(4) S. Ho and W. A. Noyes Jr., J. Am. Chem. Soc., 89, 5091 (1967).
(5) T. W. Eder and R. W. Carr Jr., J. Phys. Chem., 73, 2074 (1969).
(6) P. M. Kelley and W. L. Hase, Chem. Phys. Lett., 35, 57 (1975).
(7) A. N. Strachan and W. A. Noyes Jr., J. Am. Chem. Soc., 76, 3258 (1954).
(8) G. A. Taylor and G. B. Porter, J. Chem. Phys., 36, 1353 (1962).
(9) A. N. Strachan and D. E. Thornton, Can. J. Chem., 46, 2353 (1968).
(10) R. L. Russel and F. S. Rowland, J. Am. Chem. Soc., 92, 7508 (1970).
(11) R. N. Dixon and G. H. Kirby, Trans. Faraday Soc., 62, 1406 (1966).
(12) J. W. Rabalais, J. M. McDonald, V. Scherr, and S. P. McGlynn, Chem. Rev., 71, 73 (1971).
(13) A. H. Laufer and R. A. Keller, J. Am. Chem. Soc., 93, 61 (1971).
(14) H. Basch, Theor. Chim. Acta, 28, 151 (1973).
(15) J. E. Del Bene, J. Am. Chem. Soc., 94, 3713 (1972).
(16) C. E. Dykstra and H. F. Schaefer III, J. Am. Chem. Soc., 98, 2689 (1976).
(17) P. Pendergast and W. H. Fink, J. Am. Chem. Soc., 98, 648 (1976).
(18) E. R. Davidson, Chem. Phys. Lett., 21, 565 (1973).
(19) The GRHF program was coded by Iwata and Morokuma for the Rochester version of the GAUSSIAN 70 program (W. J. Hehre, W. A. Lathan, R. Ditchfield, M. D. Newton, and J. A. Pople, Program No. 236, QCPE, Indiana University, 1973).
(20) G. Herzberg, "Electronic Spectra of Polyatomic Molecules", Van Nostrand, Princeton, N.J., 1967.

(21) G. Herzberg, "Spectra of Diatomic Molecules", Van Nostrand, Princeton, N.J., 1950.
(22) S. V. O'Neil, H. F. Schaefer III and C. F. Bender, *J. Chem. Phys.*, **55**, 162 (1971).
(23) Strictly speaking, the GRHF orbital of the excited state is not orthogonal to the corresponding ground-state wave function of the same symmetry. Therefore, the actual $^1A'$ state of the singlet bent out of plane will have somewhat higher energy than that presented here.

(24) (a) K. Morokuma, *J. Chem. Phys.*, **55**, 1236 (1971); (b) S. Iwata and K. Morokuma, *J. Am. Chem. Soc.*, **95**, 7563 (1973); (c) K. Kitaura and K. Morokuma, *Int. J. Quantum Chem.*, **10**, 325 (1976).
(25) (a) K. Morokuma, *Acc. Chem. Res.*, **10**, 294 (1977); (b) S. Nagase and K. Morokuma, *J. Am. Chem. Soc.*, **100**, 1666 (1978).
(26) V. P. Zabransky and R. W. Carr, Jr., *J. Am. Chem. Soc.*, **98**, 1130 (1976).
(27) E. R. Davidson, *J. Am. Chem. Soc.*, **99**, 397 (1977).

Asymmetric Catalysis with Chiral Complexes of Rhodium–O-Isopropylidene-2,3-dihydroxy-1,4-bis(diphenylphosphino)-butane. 6. On the Mechanism of Reduction of (E,Z)-α-Acylaminocinnamic Acids with Homogeneous Rhodium Catalysts

Christian Detellier, Georges Gelbard, and Henri B. Kagan*

Contribution from The Laboratoire de Synthèse Asymétrique, LA CNRS No. 040-255-02, Université de Paris Sud, 91405 Orsay, France. Received January 4, 1978

Abstract: The stereochemistry of reduction of several α-acylaminocinnamic acids was investigated, in the presence of rhodium-O-isopropylidene-2,3-dihydroxy-1,4-bis(diphenylphosphino)butane (DIOP) catalyst. Cis addition on the Z isomer was demonstrated by using deuterium. Catalytic deuteration of the E isomer gives a mixture of diastereoisomers d_2. This result was interpreted as an indication of some E-Z isomerization prior to reduction, allowing calculation of the actual optical yield. Tentative mechanisms for the E-Z isomerization which do not lead to d_3 species are discussed.

Asymmetric synthesis of α-amino acids was recently realized with great efficiency by using Wilkinson-type catalysts modified by chiral phosphines.[1-7] Several attempts were made to analyze the origin of the asymmetric induction with DIOP (**1**) as the chiral ligand.[8,9] Several pieces of information were
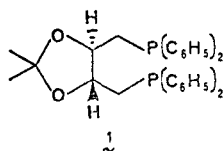
collected[9-11] but a detailed mechanism was still missing. It would be important to know the basic features of the catalytic cycle since α-amino acid precursors are very special substrates bearing two polar functions, and great care must be taken if they are to be compared with simple olefins such as cyclohexene. A better understanding of the mechanism would allow the synthesis of more efficient chiral ligands.

We examined the catalytic reduction of α-acylaminocinnamic acids **2** in experimental conditions used for asymmetric catalysis with Rh–DIOP catalysts, trying to demonstrate the stereochemistry of the reaction and eventually to detect a regiospecificity for the first hydrogen addition on the double bond. The catalyst was prepared as usual[1] in situ from ((RhCl(ethylene)$_2$)$_2$ with 2 equiv of DIOP. A benzene–ethanol (1:3) mixture was used as solvent. Several catalytic species can coexist, the more likely RhClDIOP,S and (RhDIOP,S)-$^+$Cl,[11] S being the solvent or a polar function of the substrate. We will arbitrarily adopt the formula (RhDIOP,S)$^+$ (**4**) to describe the initial species of the catalytic cycle (Scheme I) since cationic complexes give almost the same optical yields as the in situ catalyst.[11,12] The routes **4 → 5 → 6** and **4 → 7 → 6** are in competition; the former is preferred for the Wilkinson catalyst[13] but the latter fits better with recent results[14] on cationic rhodium complexes with chelating diphosphines.

Scheme I. Accepted Mechanism of Reduction by Wilkinson-Type Catalysts
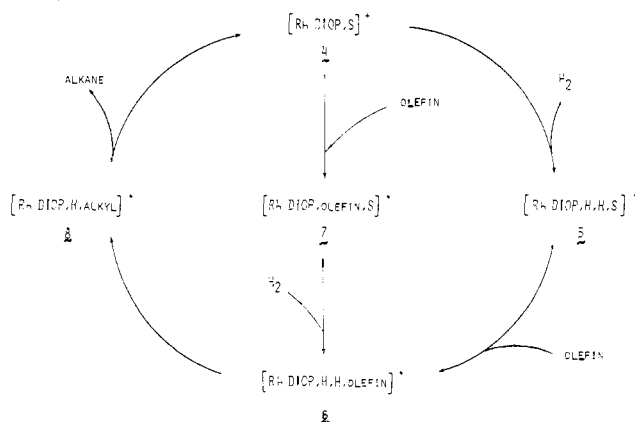
Asymmetric reduction of various E-Z isomers frequently shows a great difference in stereospecificity.[7c] With α-amino acid precursors a faster reaction and a higher optical yield were observed for the Z isomer.[9] For example, with the Rh-(+)-DIOP catalyst **2a** (Z isomer) gives (S)-N-benzoylphenylalanine (**3a**) with 70% ee, while **2a** (E isomer) gives the S configuration also, with an optical yield of 25%. This result was taken as an argument that asymmetric induction does not occur after the formation of alkylrhodium complex **8**.[9] A fast equilibrium between **8** and **6** is also excluded since it will render unimportant the olefin stereochemistry. However, no quantitative information is available on the relative rate constants of the various elementary reactions involved in the catalysis.

The stereochemistry of hydrogen addition has been established in several cases.[13a,15] From these results it is usually assumed that all other reductions are cis additions. More recently cis reduction of (Z)-**2a** catalyzed by RhCl(PPh$_3$)$_3$ was demonstrated by Kirby.[16] Since the Rh–DIOP system is very